THE EFFECT OF H_2 PURITY ON THE COMBUSTION, PERFORMANCE, EMISSIONS AND ENERGY COSTS IN AN SI ENGINE

Habib GÜRBÜZ

Department of Automotive Engineering, Faculty of Engineering, Süleyman Demirel University Isparta, Turkey.

* Corresponding author; E-mail: habibgurbuz@sdu.edu.tr

This paper aims to examine the effect of hydrogen purity on the combustion, performance, NOx emissions and energy costs in a spark ignition (SI) engine. In accordance with this purpose, two commercial hydrogen gases of different purity (i.e. 99.998 % and 99.995 %), were used as fuel in an SI engine. The engine was operated under a lean mixture (ϕ = 0.6) and wide-open throttle conditions (WOT) at 1400, 1600 and 1800 rpm engine speeds. It was found that high purity hydrogen improves engine performance parameters (i.e. indicated power, torque, thermal efficiency and specific fuel consumption) in the range of 2.4 -1.9 % depending on engine speed. The combustion duration and the cyclic variations were also decrease when the engine is operated with high purity hydrogen. However, NO_x emissions increase depending on engine speed in the range of 3.4 - 2.9 % when high purity hydrogen is used as a fuel. In addition, energy costs with high purity H_2 increase in the range of 5.9-6.5 % depending on engine speed.

Keywords: SI engine; H_2 purity; Combustion; Engine performance; NO_x Emission; Energy costs

1. Introduction

Fossil fuels such as coal, diesel, and gasoline are rapidly being consumed. Furthermore, these fuels are polluting the environment [1]. Moreover, governments have put into effect very strict environmental legislation to counter this, as well as protecting the fast depleting available fuel reserves. They have further supported research and the use of alternative fuels [2-4]. The alternative fuels such as biodiesel, natural gas, ethanol, dimethyl ether and hydrogen in terms of energy security is topical subject for researchers in this field [5]. Hydrogen is the ideal candidate as an energy carrier for systems using energy while reducing adverse effects on our livable environment. Furthermore, hydrogen reduces dependence on imported petrol for countries without natural resources [6]. Hydrogen can be directly used in spark-ignition (SI) engines as a single fuel. Furthermore, hydrogen has a wide flammability range, so hydrogen engines can be operated on a very lean mixture with high thermal efficiency and low NO_x emissions [7]. Otherwise, the NO_x emissions increase after an equivalence ratio of 0.7 in a hydrogen SI engine [8]. The high-octane value of hydrogen allows the engine to operate at a high compression ratio, and thereby increases thermal efficiency [9]. In addition, the high diffusivity speed of hydrogen increases the mixing quality around cylinders, which increases the homogeneity of the in-cylinder charge [10]. Furthermore, hydrogen provides a complete combustion process under very lean operation conditions,

also permitting the engine to operate even in low load situations along with wide-open throttle conditions [11]. The high adiabatic flame propagation speed of hydrogen can maintain stable combustion at a lean air-fuel mixture, allowing for a higher compression ratio by reducing the probability of knock and decrease cycle-by-cycle variations in the flame propagation period [12]. The lower ignition energy of hydrogen ensures engines are ignited in a lean mixture, resulting in allowing the hydrogen engine to operate at a wider range of excess air ratio [13]. The quenching distance of hydrogen is shorter that of gasoline, which can lower hydrocarbon emissions [14]. However, the temperature required for auto ignition is considerably higher than that of conventional hydrocarbon fuels [15]. Oxides of nitrogen (NO_x) are the only unwanted emissions of hydrogen combustion. NO_x are the only contaminant component emissions of hydrogen engines. The induction technique of hydrogen plays a crucial role in determining the performance characteristics of the hydrogen engine [16]. Most hydrogen fueled SI engine research has focused on the port injection technique [11]. Port fuel injection offers higher engine efficiency, operation at more a leaner mixture, lower cyclic variation and lower NO_x emissions [17].

Hydrogen is accepted as a hopeful energy carrier due to its improved natural properties, such as a high energy density of 14.300 (J/kgK), long-term viability, environmentally friendly combustion products, and production from various sources [18]. Hydrogen is not present in a free state throughout the universe, but is in abundance in compound form, otherwise, it could react quickly with other elements. Therefore, hydrogen can be obtained either from higher energy fossil fuels or lower energy water [19]. Hydrogen can be produced directly from fossil fuels using processes such as coal gasification, partial oxidation, thermal-cracking, and methane reforming. Furthermore, hydrogen can be produced by photo-biological processes, water hermolysis photo electrolysis or photolysis and dissociating water with electrolysis [20]. However, electrical energy is required for hydrogen production with water electrolysis. The use of electrical energy produced by burning fossil fuels in the electrolysis process of water for hydrogen production reduces total costs by 35% compared to the use of electricity generated in a hydroelectric plant [21]. The purification cost of hydrogen corresponds to 40-60% of the total cost of hydrogen production, depending on the production technology used. However, the produced hydrogen can be used as internal combustion engine fuel without subjecting it to any purification treatment. Therefore, the sale price of hydrogen produced is fairly competitive with the retail price of gasoline, especially in regions where required gasoline is imported [22].

This study presents the effect of hydrogen purity on combustion, engine performance, NO_x emissions and energy cost in a spark ignition (SI) engine. Two commercial hydrogen gases of differing purity (i.e. 99.998 % and 99.995 %) were used as fuel in a SI engine. The hydrogen purity rate was compared in terms of its effect on combustion, cyclic variation, engine performance, exhaust emission and energy cost. In this context, the paper reveals the relationship between increased NO_x emissions and energy costs despite improvements in engine performance parameters using high purity H_2.

2. Experimental Setup

Experimental studies were conducted on a single-cylinder L-head type SI engine with a cylinder volume of 476 cm^3. H_2 was injected into the intake manifold of the engine at a pressure of about 5 bar that is decreased using a pressure regulator from a 200 bar H_2 tank. The engine was operated with a wide-open throttle (WOT), under lean mixture (ϕ=0.6) an 8:1 compression ratio. Experimental studies

were conducted at three different engine speeds (i.e. 1400, 1600 and 1800 rpm). The in-cylinder pressure was measured using a Kistler 6052C piezoelectric pressure transducer and its charge amplifier (Kistler 5018A). The crank angle and TDC positions were encoded by using a shaft encoder (Kistler 2618B) producing 1800 pulses per revolution. H_2 and air flow rates were measured via Aalborg GFC67 and GFM77 types thermal mass flow meters, with the equivalence ratio (ϕ) being calculated. The ignition timing and injection duration were controlled via an engine control unit (Motec-M4). The intake air temperature was maintained at a constant value of 30 °C using a PIC temperature controller during the experimental studies. Inlet air pressure was measured using a Motec-M4 engine control unit and a manifold absolute pressure sensor (MAP) during the experimental studies. The outlet shaft of the engine was coupled to a hydraulic dynamometer, and the engine speed was changed by varying the engine load. The probe of an emission analyzer (IMR 1400-C) was connected in a perpendicular position to the exhaust flow of the engine, and NO_x emissions, excess O_2 and exhaust gas temperature were measured. Fig.1 shows a schematic diagram of the experimental set-up.

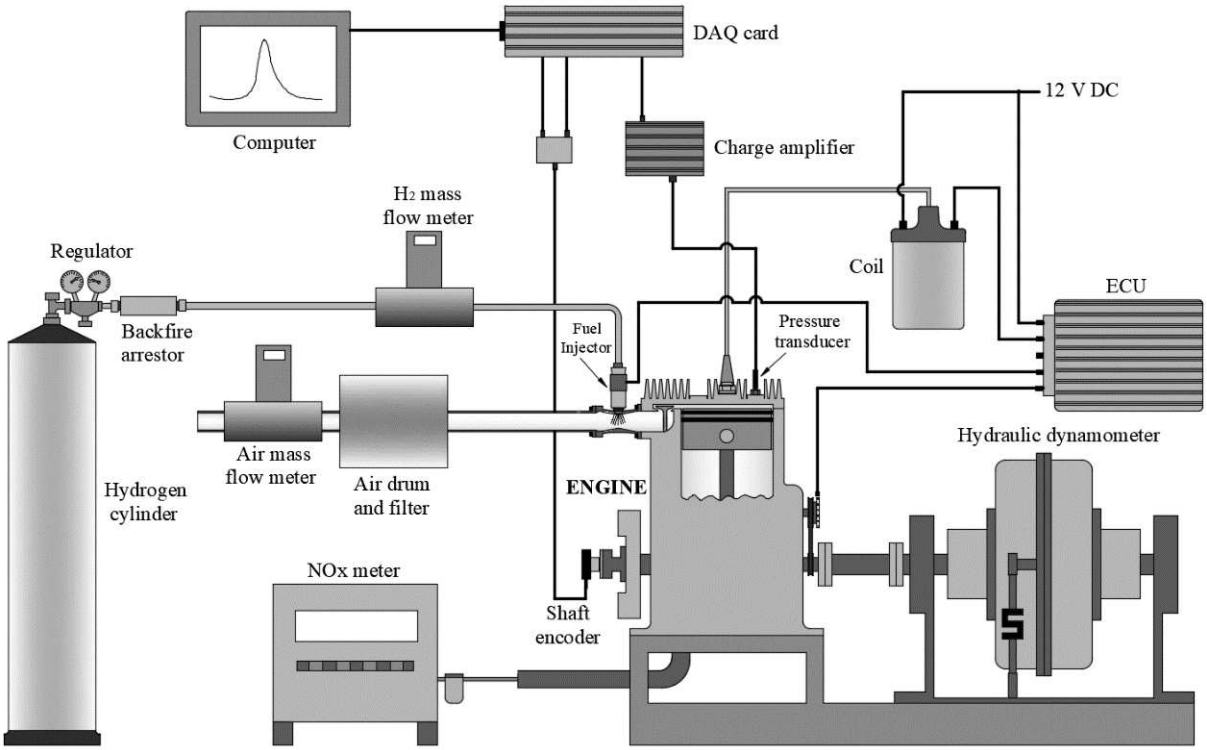

Fig.1. Schematic diagram of experimental set-up

A DAQ card (Measurement Computing-USB-1616HS-4) was connected to collect to the crank angle sensor and pressure transducer signals. The stored data on a PC computer was analyzed in order to calculate the engine and combustion parameters. For every working condition, 50 consecutive combustion cycles were operated in order to derive the corresponding 'mean cycles' to the cylinder pressure data. The data obtained was used to calculate real time engine performance parameters [i.e. indicated thermal efficiency (η_i), indicated power (P_i), indicated torque (T_i), indicated specific fuel consumption (sfc_i)] and combustion parameters [i.e. indicated mean effective pressure (*imep*) and mass fraction burned (*mfb*)].

The mass fraction burned (*mfb*) was calculated using an equation developed by Matekunas [23]. In the equation, the pressure ratio is defined as the ratio of the cylinder pressure from a firing cycle $P(\theta)$ and the corresponding motored cylinder pressure $P_o(\theta)$:

$$PR(\theta) = \frac{P(\theta)}{P_o(\theta)} - 1 \quad (1)$$

After this, the pressure ratio (*PR*) is normalized by its maximum value:

$$PR_N(\theta) = \frac{PR(\theta)}{PR(\theta)_{\max}} \quad (2)$$

In one paper in which the number of cycles was determined to calculate the cyclic variation, Gürbüz et al. (2014) found that COVimep increases linearly up to 50 consecutive combustion cycles and that there is an extremely small increase in COV_{imep} (3%) after 50 cycles [24]. Therefore, the 50 consecutive combustion cycles were used to determine the cyclic variation in this paper. The cyclic variation of the combustion cycles was calculated from the in-cylinder pressure data using the coefficient of variation of *imep* (COV_{imep}) as given in Eq.3 [25]:

$$COV_{imep} = (\sigma_{imep} / imep_{mean}) \times 100 \quad (3)$$

In this paper, two different commercial H_2 gases were used in industrial classification, defined as Hydrogen 4.6 (Purity> = 99.996%) and Hydrogen 5.0 (Purity> = 99.999%). In order to distinguish from between each hydrogen gas, Hydrogen 4.6 is defined as pure hydrogen and Hydrogen 5.0 is defined as high purity hydrogen. An elemental analysis of the commercial H_2 gas of two different purities used as engine fuel in this paper is given in Table 1. The cost of the H_2 gas for Turkey is given in Table 2.

Table 1. Commercial H_2 purity and other gas components

Component	Unit	High purity H_2	Pure H_2
H_2	%	99.998	99.995
N_2	ppm	13.097	29.778
O_2	ppm	0.49	4.82
Moisture	ppm	1.7	5.43

Table 2. Cost of H_2 gas for Turkey

H_2 purity	Tank water capacity (liter)	Tank H_2 pressure (bar)	Tank H_2 capacity (m^3)	H_2 cost ($) + taxes for Turkey (8.2 m^3)	H_2 cost ($) + taxes for Turkey (liter)
High purity H_2	50	200	8.2	197.986	0.0241
Pure H_2	50	200	8.2	182.147	0.0222

2.1. Error analysis

An error analysis of the calculated (i.e. indicated power, indicated thermal efficiency, indicated specific fuel consumption, volumetric efficiency, and equivalence ratio,) and measured values (engine speed, in-cylinder pressure, crank angle, fuel flow, air flow NO_x, O_2 and exhaust gas temperature) was predicted using Eq.4.

$$\Delta R = \left[\left(\frac{\partial R}{\partial x_1} \Delta x_1 \right)^2 + \left(\frac{\partial R}{\partial x_2} \Delta x_2 \right)^2 + \ldots + \left(\frac{\partial R}{\partial x_n} \Delta x_n \right)^2 \right]^{1/2} \quad (4)$$

The accuracy of the measurement equipment used in this paper is given in Table 3. Error analysis of the measured parameters is given in Table 4.

Table 3. Accuracy values of the measurement equipment

Variable	Device	Accuracy	
In-cylinder pressure	Kistler 6052C	± 0.4 % AR*	-
Crank angle	Kistler 2618B	± 0.02°	-
Air flow rate	Aalborg GFM77	± 1.5% FS*	± 0.48**
Hydrogen flow rate	Aalborg GFC67	± 1.5% FS*	± 0.24**
Engine speed	Mag. Pick-up	± 6 rpm AR*	-
Exhaust Emission	IMR 1400 Compact	NO_x : ± 80 ppm FS*	-
		O_2 : ± 0.2 % FS*	-
		Temperature : ± 1 °C FS*	-

* FS: Full scale, AR: All range ** Accuracy of device in measurement range

Table 4. An error analysis of the measured and calculated parameters in this paper

Engine Parameters	Calculated Values at 1600 rpm	Error	Percentage (%)
P_i	2.813 kW	0.0159 kW	0.565
η_i	21.977 %	0.142 %	0.646
sfc_i	136.509 g/kWh	0.824 g/kWh	0.603
Volumetric efficiency	81.12 %	0.608 %	0.749
Equivalence ratio	0.6	0.0015	0.250
NO_x	1099 pp	10 ppm	0.910
O_2	7.71 %	0.028 %	0.363
$T_{exhaust\ gas}$	364.8 °C	0.304 °C	0.835

3. Result and Discussion

Fig.2. shows the variation of N_2, O_2 and moisture values versus the H_2 purity rate for three different engine speeds. The components of the fuel gas (i.e. pure and high purity H_2) were calculated considering the amount of H_2 taken into the cylinder for each engine speed according to the data in Table 1. The amount of moisture in the fuel is the most important factor affecting the flammability of the fuel. Moisture acts as a heat sink due to the evaporation of water, thus reducing the amount of oxygen in the combustion zone by diluting with flammability volatiles [26]. Under normal atmospheric conditions, nitrogen is an inert gas, and thus nitrogen is not significantly affected by the reaction [25]. Therefore, the nitrogen acts as a heat sink, such as moisture in the combustion reaction,

and reduces the combustion temperature. In other words, the combustion reaction is significantly influenced from by the amount of nitrogen. As a result of this, the increase in the amount of moisture and nitrogen in the fuel reduces the flammability of the fuel and causes a decrease in the engine performance parameters. It can be seen in Fig.2 that the N_2, O_2 and moisture increased 2.27, 9.46 and 3.19 %, respectively, with pure H_2 according to the high purity H_2. Generally, the increase in the amount of moisture and nitrogen in the pure H_2 significantly influenced the results of this paper (i.e. in-cylinder combustion, engine performance parameters and exhaust NO_x emissions).

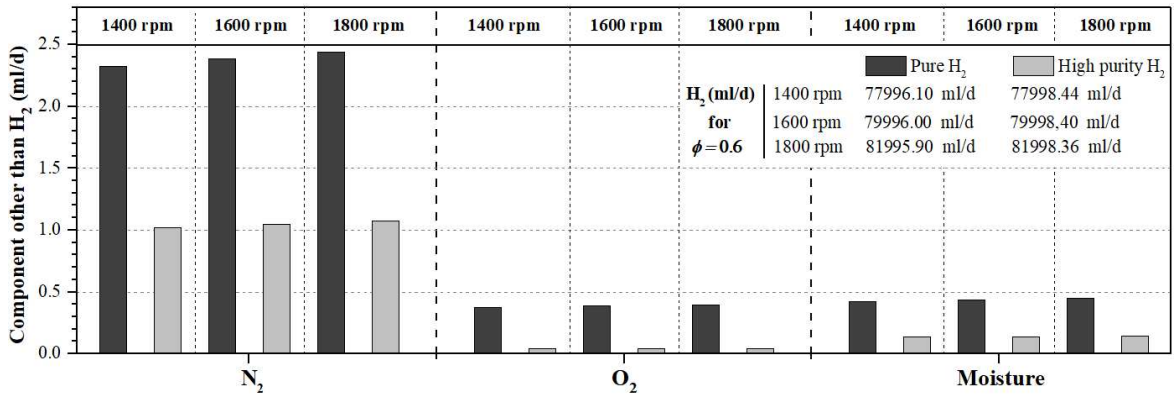

Fig.2. Variation of N_2, O_2 and moisture values versus H_2 purity rate for the three engine speeds

The variation of *imep* versus different spark ignition timings for the three engine speeds is given in Fig. 3. As shown in Fig. 3, the indicated mean effective pressure (*imep*) increases at the optimum ignition timing (MBT-minimum ignition advance for best torque) when the engine is operated with high purity H_2 for each of the three engine speeds. As shown in Fig.3, the mean effective pressure (imep) value at the MBT increases with the use of of high purity hydrogen for each of the three engine speeds. However, when the ignition timing was shifted from MBT timing to the TDC (retard ignition timing), the increase in the *imep* produced using high purity hydrogen is further increased. In contrast, when the ignition timing is shifted from MBT time to an expansion stroke (advance ignition timing), the increase in the *imep* produced using high purity hydrogen decreases, and the pure hydrogen become even more advantageous than the high purity hydrogen. This result is probably due to the fact that sufficient time for combustion, in the case of an over advanced position, compensates for the faster burning ability of high purity H_2. However, these conditions do not eliminate the positive effect of high purity H_2 at the MBT in terms of engine performance. However, the optimum ignition timing, corresponding to MBT, gets closer to TDC with high purity H_2. This effect is greater at low engine speeds (i.e. 1400 rpm), and even almost disappears at the high engine speeds (i.e. 1800 rpm). Following these results, MBT has been used to in the investigation of combustion, engine performance, exhaust emission and energy costs in this paper.

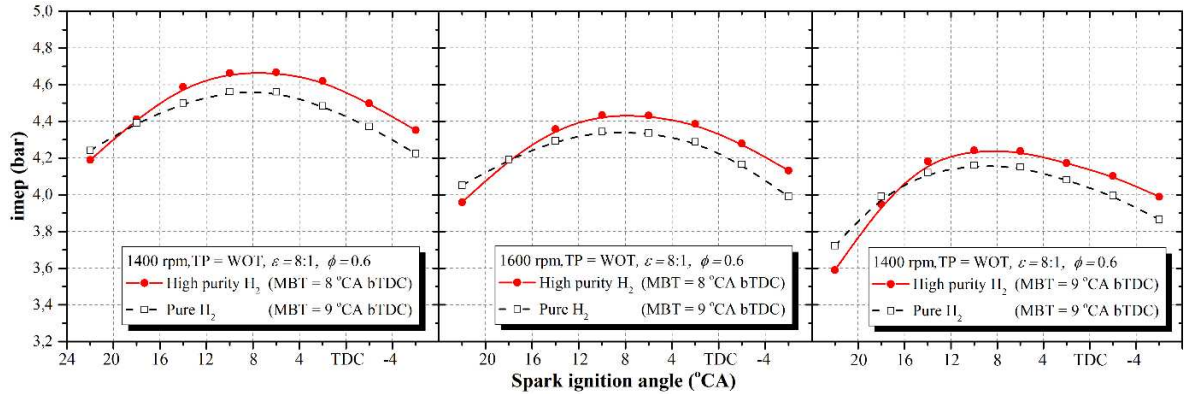

Fig.3. Variation of *imep* versus different spark ignition timings for three engine speeds

Fig.4(a) illustrates the profiles of in-cylinder pressure versus crank angle for three different engine speeds. In-cylinder pressure profiles were created by calculating the average of 50 consecutive combustion cycles. Engine speed increased with a reduction of engine output shaft load which caused a decrease of maximum pressure (P_{max}) for both H_2 purity rates, as shown in Fig.5. Furthermore, the combustion pressure curves split earlier from the motoring curve when the engine was operated with high purity H_2 for each of the three engine speeds. Furthermore, the position of P_{max} (φ_{Pmax}) got closer to TDC with high purity hydrogen for each of the three engine speeds. P_{max} increased approximately in the range of 1.43 - 0.85 bar using high purity hydrogen, while engine speed changed between 1400-1600 rpm. The MBT ignition timing approached even closer to TDC with high purity hydrogen for each of the three engine speeds. Fig.4(b) shows the profiles of the in-cylinder pressure increase rate versus crank angle for the three different engine speeds. Fig.4(b) shows the maximum rate of pressure rise (MRPR) raised when the engine was operated with high purity H_2. It can be seen that the MRPR decreased for both H_2 purity rates due to a reduction of in-cylinder pressure and temperature as a result of increasing engine speed. The increase in the MRPR was approximately 11.2%, 9.8% and 7.4% at engine speeds of 1400, 1600, and 1800 rpm, respectively, when the engine was operated using high purity H_2. The highest MRPR was obtained at 1400 rpm, when the engine was operated with high purity H_2. However, this value is less than the 2.6 bar/°CA which is the knock limit of the SI engine.

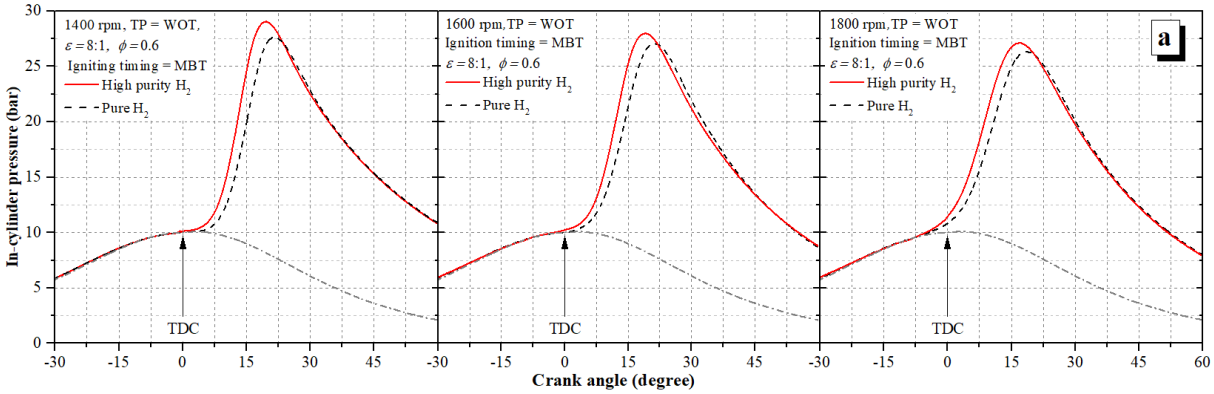

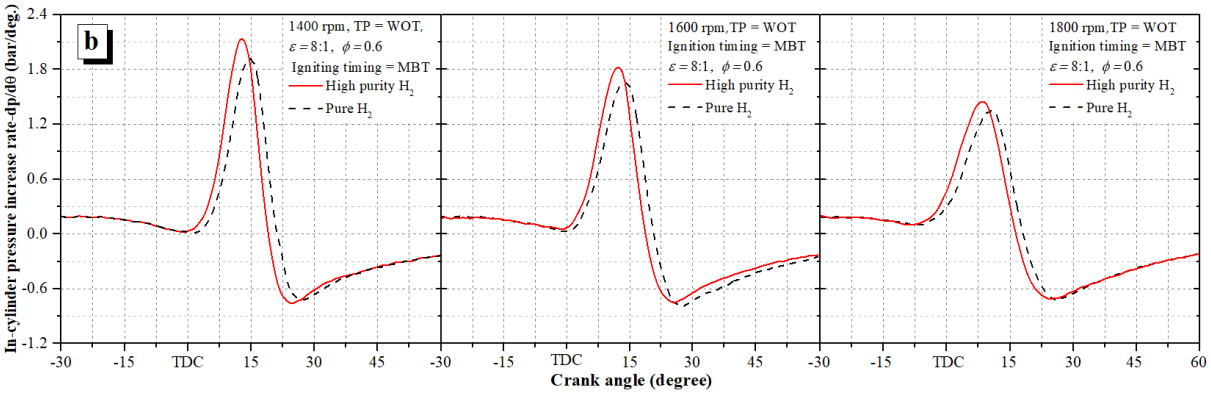

Fig.4. Variation of **(a)** cylinder pressure and **(b)** rate of pressure rise versus H_2 purity for the three engine speeds

The variation of P_{max} and θ_{Pmax} versus the H_2 purity for the three engine speeds is given in Fig.6. According to Fig. 5, P_{max} increased by approximately 5.2%, 3.4% and 3.1% at engine speeds of 1400, 1600, and 1800 rpm, respectively, when the engine was operated with high purity H_2. Moreover, θ_{Pmax} decreased by about 8.1%, 6.3% and 5.7% at engine speeds of 1400, 1600, and 1800 rpm, respectively, when operated with high purity H_2. These results appear as a result of an increased burning speed along with an increasing purity rate. The decrease in the effect on the pressure parameters of H_2 purity with engine speed, can be explained by the contribution of the in-cylinder turbulence to the increase in combustion speed.

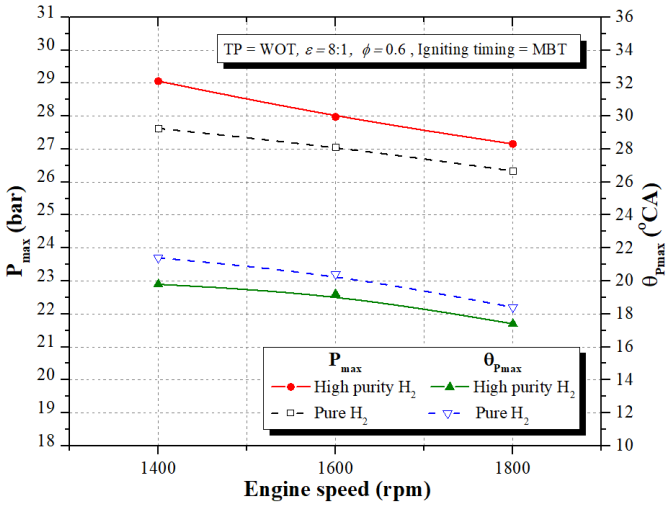

Fig.5. Variation of P_{max} and θ_{Pmax} versus H_2 purity for the three engine speeds

In-cylinder combustion in spark ignition engines can be divided into three basic parts, defined depending on the crank angle, as the flame initiation period, the flame propagation period and the flame termination period [27]. Flame development and propagation duration are dealt with as two important factors influencing SI engine thermal efficiency [28]. The variation of *mfb* curves, according to the crank angle after ignition for the two H_2 purities at the three different engine speeds, is given in Fig.6. In addition to the crank angle positions for *0-10 % mfb*, *10- 90 % mfb*, *100 % mfb* as well as *90*

% mfb are listed in Table 5. In Fig.6, since the ignition timings corresponding to MBT for pure hydrogen and high purity hydrogen have changed, the mfb curves are given according to the normalized crank angle (crank *angle after ignition*). Therefore, it is possible to read the results given in Table 5 through Fig.6. Fig.6 shows that the *0-10% mfb* (flame initiation period), *10-90% mfb* (flame propagation period) and *90-100% mfb* shorten when high purity hydrogen is used as fuel. This shortening as the crank angle is higher in the flame initiation period than in the other two combustion periods, as shown in comparison to the burn angles given in Table 5. The fast burning property of hydrogen increases with an increase in purity, and this effect becomes more dominant in the flame development angle, which is the slowest phase of combustion. The reduction in the total combustion duration is about 8.44%, 7.48% and 6.20% at engine speeds of 1400, 1600, and 1800 rpm, respectively, when engine is operated with high purity H_2. The increase of engine speed causes an increase flame speed as a result of the increase in cylinder turbulence. The increased heat-release rate, with the effect of high turbulence, causes an increase in *mfb*. Therefore, the effect of the hydrogen purity to the combustion duration is lower along with increased engine speeds. However, it is obvious that hydrogen purity contributes to the shortening of the combustion periods in addition to the increasing turbulence effect along with the increase in engine speed. Moreover, the effect of hydrogen purity on the flame termination period appears to be almost nonexistent. On the other hand, in-cylinder turbulence, which increases with engine speed, is also effective in the final flame period.

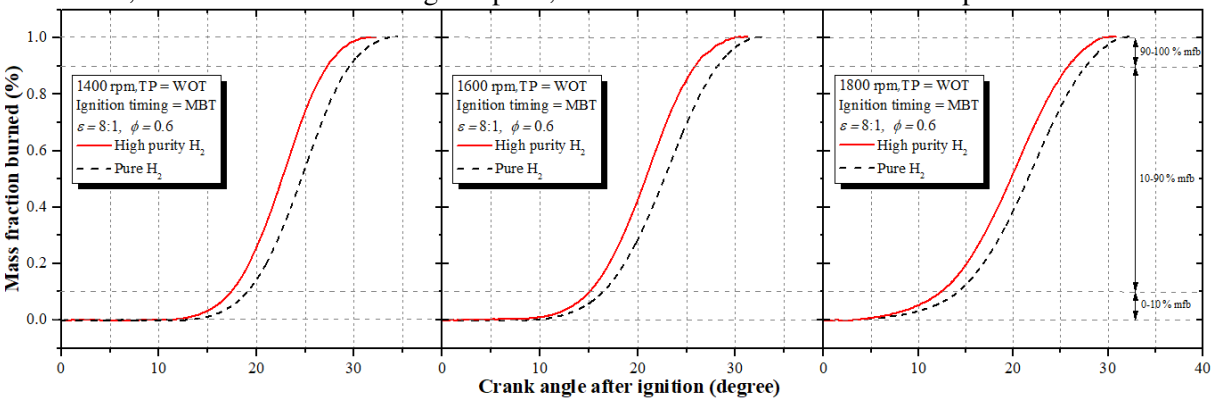

Fig.6. Variation of *mfb* versus H_2 purity for different engine speeds

Table 5. Crank angle positions of combustion phase (*mfb*) versus H_2 purity for the three engine speeds

Engine speed (rpm)	θ_i - θ_{10} *mfb*			θ_{90} *mfb*		θ_{10} - θ_{90} *mfb*			θ_{100} *mfb*		θ_{90} - θ_{100} *mfb*			Difference in total combustion durations (%)
	$H_{2\text{-}p}$ (°CA)	$H_{2\text{-}hp}$ (°CA)	Difference (%)	$H_{2\text{-}p}$ (°CA)	$H_{2\text{-}hp}$ (°CA)	$H_{2\text{-}p}$ (°CA)	$H_{2\text{-}hp}$ (°CA)	Difference (%)	$H_{2\text{-}p}$ (°CA)	$H_{2\text{-}hp}$ (°CA)	$H_{2\text{-}p}$ (°CA)	$H_{2\text{-}hp}$ (°CA)	Difference (%)	
1400	19.0	17.4	10.34	29.4	27.2	10.4	9.8	6.12	33.4	30.8	3.8	3.6	5.5	% 8.44
1600	16.4	15.0	9.33	28.4	26.0	11.6	11.0	5.45	31.6	29.4	3.4	3.4		% 7.48
1800	13.8	12.6	9.52	27.6	25.8	13.8	13.2	4.54	30.8	29.0	3.2	3.2		% 6.20

Cyclic combustion variability is one of the main characteristics which affect the performance of SI engines. A cyclic variability above 10% significantly affects engine output power [24]. The variation of COV_{imep} versus H_2 purity for the three engine speeds is given in Fig.7. In this paper, 50 consecutive combustion cycles are used while the COV_{imep} is calculated. It can be seen in Fig.7 that the COV_{imep} increases with increasing engine speed for both H_2 purities. However, COV_{imep} decreases with increasing H_2 purity for the three engine speeds. The reduction in COV_{imep} is approximately 6.5%,

4.2% and 3.3% at engine speeds of 1400, 1600, and 1800 rpm, respectively, when the engine is operated with high purity H_2. This result shows that engine operation is more stable when operated with high purity hydrogen. As a result, we can say that stable engine operation contributes to the improvement of the engine performance parameters as given in Fig.8.

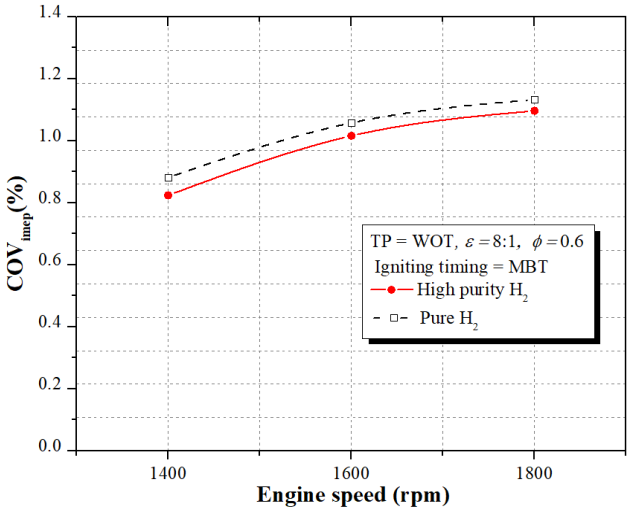

Fig.7. Variation of COV_{imep} versus H_2 purity for three engine speeds

Fig. 8 illustrates the variation of indicated power (P_i), indicated thermal efficiency (η_i), indicated torque (T_i) and indicated specific fuel consumption (sfc_i) versus H_2 purity for the three engine speeds. P_i, η_i and T_i increased with increasing H_2 purity, while sfc_i decreased. As can be seen in Fig.8, IP, IT and ITE, owing to increasing H_2 purity, increased by approximately 2.4%, 2.1%, and 1.9% at engine speeds of 1400, 1600, and 1800 rpm, respectively, while *ISFC* decreased at the same rates. The obtained improvement in the engine performance parameters using the high purity H_2, appeared as a result of the imep, which is increased by the effect of in-cylinder pressure and temperature.

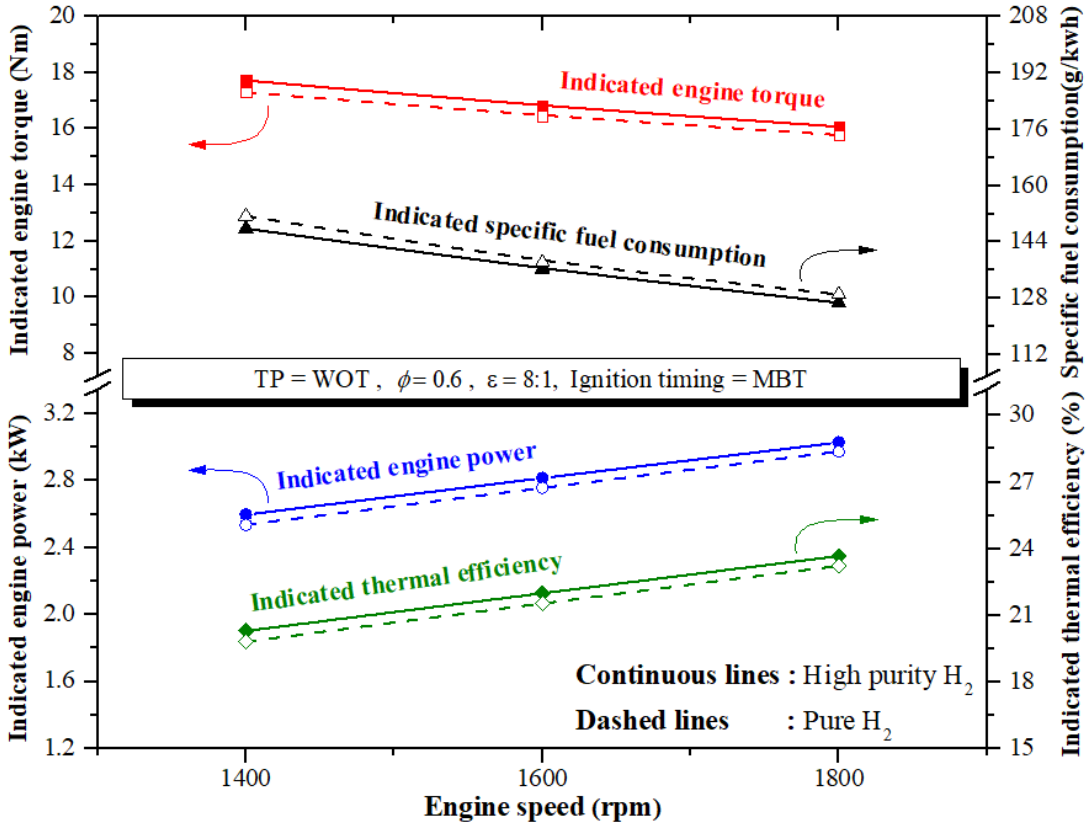

Fig.8. Variation of P_i, η_i, T_i and sfc_i versus H_2 purity for the three engine speeds

The variation of exhaust NO_x emissions versus H_2 purity for the three engine speeds is given in Fig 9 (a). As a result of increasing engine speed, exhaust NO_x emissions decreased for both H_2 purity rates due to a reduction of in-cylinder pressure and temperature. As can be seen in Fig.9 (a), exhaust NO_x emissions are increased about 3.4%, 3.1%, and 2.9% at engine speeds of 1400, 1600, and 1800 rpm, respectively, when the engine is operated with high purity H_2. On the other hand, the P_{max} is closer to TDC with high purity H_2 forming more time to recycle NO_x emissions in the expansion stroke. However, the cooling effect caused by the faster expansion causes the NO_x reactions to freeze and the concentration in the exhaust gases to increase. This effect can be seen from the shapes of the pressure curves in Fig.4. However, the amount of excess O_2 in the exhaust gases decreases due to the increase of NO_x emissions as shown in Fig.9 (b). Moreover, the exhaust gas temperature changes very little with increasing H_2 purity, as shown in Fig. 9 (c). This is because, combustion slides towards the expansion stroke when the engine is operated with pure H_2, and the exhaust gas temperature increases slightly, as shown in Fig.9 (c).

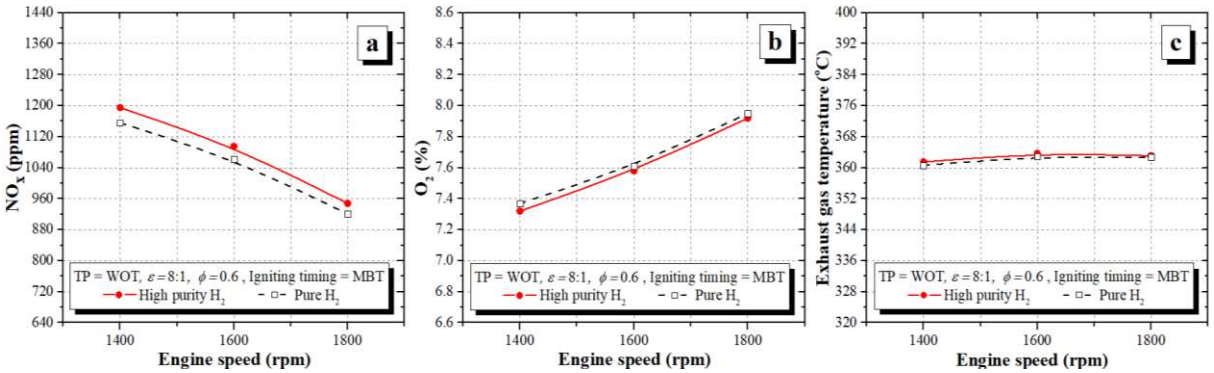

Fig.9. Variation of **(a)** NO_x, **(b)** O_2 and **(c)** exhaust gas temperature versus H_2 purity for the three engine speeds

Fig. 10 shows the variation of energy costs versus H_2 purity for the three engine speeds. The energy costs are calculated considering the generated indicated power against the amount of hydrogen taken into the cylinder for each engine speed. The energy costs increase by approximately 5.9%, 6.2%, and 6.5% at engine speeds of 1400, 1600, and 1800 rpm, respectively, when the engine is operated with high purity hydrogen. It can be seen that the increasing energy costs and exhaust NO_x emissions, despite increasing engine power, lead to a reduction in overall system efficiency when the engine is operated with high purity hydrogen. However, high purity H_2 can be selected to increase the performance of the hydrogen engine, despite high exhaust emissions and energy costs. Furthermore, the price of hydrogen varies from country to country due to the influence of many factors (i.e. production and purification method of H_2, legal taxes, and shipping fees). Therefore, the results shown in Fig.10 may vary from country to country.

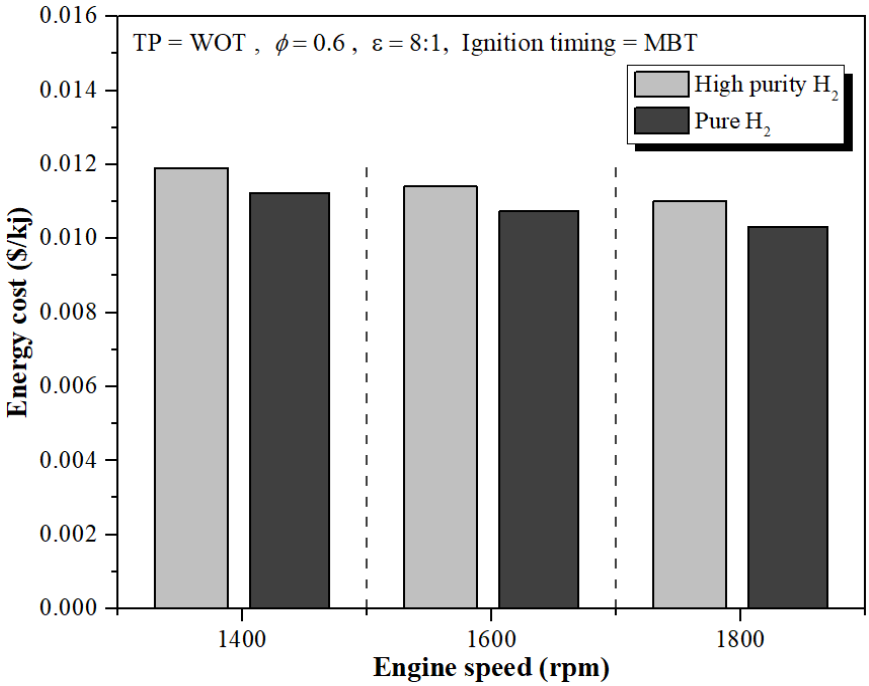

Fig.10. Variation of energy cost versus H_2 purity for the three engine speeds

4. Results

This paper seeks, at different engine speeds, to ascertain the effect of hydrogen purity on combustion, engine performance, NO_x emissions and energy costs in a SI engine. The conclusions of the study are as follows:

- *imep* increased at the MBT with high purity H_2 for each the three engine speeds. Moreover, MBT came closer to TDC (towards retard position) with high purity H_2.
- P_{max} increased approximately 5.2%, 3.4% and 3.1% at engine speeds of 1400, 1600, and 1800 rpm, respectively, when the engine is operated with high purity H_2. Moreover, θ_{Pmax} decreased about 8.1%, 6.3% and 5.7% at engine speeds of 1400, 1600, and 1800 rpm, respectively, with high purity H_2.
- The total combustion duration decreased by approximately 8.44%, 7.48% and 6.20% at engine speeds of 1400, 1600, and 1800 rpm, respectively, with high purity H_2. Moreover, the COV_{imep} decreased by approximately 6.5%, 4.2% and 3.3% at engine speeds of 1400, 1600, and 1800 rpm, respectively, with high purity H_2.
- Engine performance parameters (i.e. indicated power, torque, thermal efficiency and specific fuel consumption) improved by approximately 2.4%, 2.1%, and 1.9% at engine speeds of 1400, 1600, and 1800 rpm, respectively, with high purity H_2.
- NO_x emissions increased by approximately 3.4%, 3.1%, and 2.9% at engine speeds of 1400, 1600, and 1800 rpm, respectively, with high purity H_2. Moreover, the amount of excess O_2 in the exhaust gases decreased depending on increasing NO_x emissions.
- As a general result, the increase in the amount of moisture and nitrogen in the pure H_2 according to the high purity H_2, negatively influenced the results of this paper (i.e. in-cylinder combustion, engine performance parameters and exhaust NO_x emissions).
- Furthermore, the energy costs increased by approximately 5.9%, 6.2%, and 6.5% at engine speeds of 1400, 1600, and 1800 rpm, respectively, with high purity H_2. However, it can be said that high purity H_2 as a fuel can be preferred to increase the performance of the hydrogen engine, despite high exhaust emissions and energy costs.

References

[1] Alazemi, J. and Andrews, J. Automotive hydrogen fueling stations: An international review. Renew. Sustain. Energy Rev. 2015;48:483-499.

[2] Ganesh, R.H., Subramanian, V., Balasubramanian, V., Mallikarjuna, J.M., Ramesh, A., and Sharma, R.P. Hydrogen fueled spark ignition engine with electronically controlled manifold injection: An experimental study. Renewable Energy 2008;33(6):1324-1333.

[3] Verhelst, S., Verstraeten S. and Sierens. R. A Comprehensive Overview of Hydrogen Engine Design Features. J. Automobile 2005;221(8):911-920.

[4] Balat, M. Potential importance of hydrogen as a future solution to environmental and transportation problems. Int. J. Hydrogen Energy 2008;33(15):4013-4029.

[5] Korakiznitis, T., Namasivayam, A.M. and Crookes R.J. Natural-gas fueled spark ignition (SI) and compression-ignition (CI) engine performance and emissions. Prog. Energy Combust. Sci. 2011; 37:89–112.

[6] Sakintunaa, B., Lamari-Darkrimb, F. and Hirscherc M. Metal hydride materials for solid hydrogen storage: A review. Int. J. Hydrogen Energy 2007;32(9) 1121-1140.

[7] Ghazal, O.H. Performance and combustion characteristic of CI engine fueled with hydrogen enriched diesel. Int J Hydrogen Energy 2013;38(35):15469-15476.

[8] Sakthınathan, G.P. and Jeyachandran, K. Theoretical and experimental validation of hydrogen fueled spark ignition engine. Thermal Science 2010;14(4): 989-1000.

[9] Ji, C., Wang, S. and Zhang B. Effect of spark timing on the performance of a hybrid hydrogen–gasoline engine at lean conditions. Int. J. Hydrogen Energy 2010;35(5):2203-2212.

[10] Salvi, B.L. and Subramanian, K.A. Sustainable development of road transportation sector using hydrogen energy system, Renew. Sustain. Energy Rev. 2015;51:1132-1155.

[11] White, C.M., Steeper, R.R. and Lutz, A.E. The hydrogen-fueled internal combustion engine: A technical review. Int. J. Hydrogen Energy 2006;31(10):1292-1305.

[12] Ma, F., Wang, Y., Liu, H., Li, Y., Wang, J. and Ding, S. Effects of hydrogen addition on cycle-by-cycle variations in a lean burn natural gas spark-ignition engine. Int. J. Hydrogen Energy 2008; 33(2):823-831.

[13] Shivaprasad, K.V., Raviteja, S., Chitragar, P. and Kumar G.N. Experimental Investigation of the effect of hydrogen addition on combustion performance and emissions characteristics of a spark ignition high speed gasoline engine. Procedia Technology 2014;14:141-148.

[14] Ceper, B.A., Akansu, S.O., Kahraman, N. Investigation of cylinder pressure for H_2/CH_4 mixtures at different loads. Int. J. Hydrogen Energy 2009;34(11): 4855-4861.

[15] Antunes, J.M.G., Mikalsen, R. and Roskilly, A.P. An investigation of hydrogen-fuelled HCCI engine performance and operation. Int. J. Hydrogen Energy 2008;33(20):5823-5828.

[16] Suwanchotchoung, N. Performance of a Spark Ignition Dual-fuelled Engine Using Split Injection Timing (Ph.D. thesis), Mechanical Engineering, Vanderbilt University, USA, 2003.

[17] Yi, H.S., Min, K. and Kim, E.S. The optimized mixture formation for hydrogen fuelled engines. Int. J. Hydrogen Energy 2000;25(7):685-690.

[18] Cipriani, G., Dio, V.D., Genduso, F., Cascia, D.L., Liga, R., and Miceli, R. Perspective on hydrogen energy carrier and its automotive applications. Int. J. Hydrogen Energy 2014;39(16): 8482-8494.

[19] Verhelst, S. Recent progress in the use of hydrogen as a fuel for internal combustion engines. Int. J Hydrogen Energy 2014;39(2):1071-1085.

[20] Alazemi J., and Andrews J. Automotive hydrogen fuelling stations: an international review. Renew. Sustain. Energy Rev. 2015;48:483-499.

[21] Steinberg, M. and Cheng, H.C. Modern and prospective Technologies for hydrogen production from fossil fuels. Int J Hydrogen Energy 1989;14(11):797-803.

[22] Gambini, M. and Vellini, M. Comparative analysis of H_2/O_2 cycle power plants based on different hydrogen production systems from fossil fuels. Int. J. Hydrogen Energy 2005;30(6): 593-604.

[23] Matekunas, F. Modes and measures of cyclic combustion variability. 1983; SAE Technical Paper 830337.

[24] Gürbüz, H., Akçay, İ.H., and Buran, D., An investigation on effect of in-cylinder swirl flow on performance, combustion and cyclic variations in hydrogen fuelled spark ignition engine, Journal of the Energy Institute, 87(1),1-10, 2014.

[25] Heywood, J.B. Internal combustion engine fundamentals, McGraw-Hill, London, U.K, 1988.

[26] Shafizadeh, F., Chin, P., and Degroot, W. Effective heat content of green forest fuels. For. Sci. 1977;23(1): 81-89

[27] Kang, K.Y. and Reitz, R.D., The effect of intake valve alignment on swirl generation in a DI diesel engine, Exp. Therm. Fluids Sci. 1999;20(2):94-103.

[28] Syred, N. A review of oscillation mechanisms and the role of the PVC in swirl combustion systems, Prog. Energy Combust Sci. 2006;32(2):93-161.

Notation

aTDC	= after top dead center (°CA)
bTDC	= before top dead center (°CA)
°CA	= crank angle (degrees)
COV_{imep}	= coefficient of variations of imep
$H_{2\text{-}p}$	= pure hydrogen
$H_{2\text{-}hp}$	= high purity hydrogen
P_i	= indicated power (kW)
Sfc_i	= indicated specific fuel consumption (g/kWh)
T_i	= indicated torque (Nm)
η_i	= indicated thermal efficiency (%)
imep	= indicated mean effective pressure (bar)
$imep_{mean}$	= mean value of imep (bar)
MBT	= maximum brake torque (Nm)
mfb	= mass fraction burned (%)
N_2	= nitrogen
O_2	= oxygen
P	= in-cylinder pressure (bar)
P_{max}	= maximum pressure (bar)
P_o	= motored cylinder pressure (bar)
ppm	= particle per million
PR	= pressure ratio (bar)
SI	= spark ignition
TDC	= top dead center
$T_{exhaust\ gas}$	= exhaust gas temperature (°C)
WOT	= wide open throttle
0–10% mfb	= flame initiation period (°CA)
10–90% mfb	= flame propagation period (°CA)
90–100% mfb	= flame termination period (°CA)
θ	= instant crank angle (degrees)
σ_{imep}	= standard deviation of imep
ϕ	= equivalence ratio
φ_{Pmax}	= position of P_{max} (°CA)